Poultry Science®

Molecular characterization of a virulent goose astrovirus genotype-2 with high mortality in vitro and in vivo

Linhua Xu,[*,†,‡] Zhen Wu,[*,†,‡] Yu He,[*,†,‡] Bowen Jiang,[*,†,‡] Yao Cheng,[*,†,‡] Mingshu Wang,[*,†,‡] Renyong Jia,[*,†,‡] Dekang Zhu,[*,†,‡] Mafeng Liu,[*,†,‡] Xinxin Zhao,[*,†,‡] Qiao Yang,[*,†,‡] Ying Wu,[*,†,‡] Shaqiu Zhang,[*,†,‡] Juan Huang,[*,†,‡] Xumin Ou,[*,†,‡,§] Di Sun,[*,†,‡] Anchun Cheng,[*,†,‡] and Shun Chen[*,†,‡,§,1]

[*]*Research Center of Avian Disease, College of Veterinary Medicine, Sichuan Agricultural University, Chengdu, Sichuan 611130, China;* [†]*Key Laboratory of Animal Disease and Human Health of Sichuan Province, Sichuan Agricultural University, Chengdu, Sichuan 611130, China;* [‡]*Engineering Research Center of Southwest Animal Disease Prevention and Control Technology, Ministry of Education of the People's Republic of China, Chengdu 611130, China; and* [§]*Key Laboratory of Agricultural Bioinformatics, Ministry of Education of the People's Republic of China, Chengdu 611130, China*

ABSTRACT Goose astrovirus (**GAstV**) is a newly identified viral pathogen threatening waterfowl, exhibiting a high prevalence across various regions in China. Notably, the Guanghan District of Deyang City, situated in Sichuan Province, has faced a outbreak of GAstV, resulting in significant mortality among goslings due to the induction of gout-like symptoms. In our research, we successfully isolated a GAstV strain known as GAstV SCG3. This strain exhibits efficient replication capabilities, proving virulent in goslings and goose embryos. Our study delved into the characteristics of GAstV SCG3 both in vitro and in vivo. Additionally, we examined tissue phagocytosis and the distribution of GAstV SCG3 in deceased goslings using H&E staining and IHC techniques. According to the classification established by the ICTV, GAstV SCG3 falls under the category of GAstV genotype-2. Notably, it demonstrates the highest homology with the published AHAU5 sequences, reaching an impressive 98%. Furthermore, our findings revealed that GAstV SCG3 exhibits efficient proliferation exclusively in goose embryos and in LMH cells, while not manifesting in seven other types of avian and mammalian cells. Significantly, the mortality of GAstV on goslings and goose embryos are 93.1 and 80%, respectively. Moreover, the viral load in the livers of infected goslings surpasses that in the kidneys when compared with the attenuated strain GAstV SCG2. The mortality of GAstV is usually between 20% and 50%, our study marks the first report of a virulent GAstV strain with such a high mortality.

Key words: goose astrovirus virulent strain, genotype-2, high mortality, in vitro and in vivo

2024 Poultry Science 103:103585
https://doi.org/10.1016/j.psj.2024.103585

INTRODUCTION

GAstV is a novel waterfowl virus that has emerged, causing gout in goslings in China since 2016 (Yang, et al., 2018), the incidence rate of GAstV among waterfowl viruses had reached 50.81% between 2018 and 2021 (He et al., 2022). GAstV had been demonstrated to be able to spread horizontally and vertically (Wei et al., 2020a). The primary hosts for transmission are goslings younger than 3 wk of age (An et al., 2020). The predominant symptom of GAstV is the substantial urate accumulation in infected goslings, which leads to gout (Zhang et al., 2018a, 2022a). The mortality of GAstV is typically ranging from 20 to 50% (Zhu et al., 2022). There have been some reports of duck-origin GAstV (Wei et al., 2020b). Besides, there have also been reports of mixed infections of other viruses with the GAstV (Bidin et al., 2012; Liu, et al., 2019). However, there is no report indicating that GAstV can cause such a high mortality, leading to a significant number of deaths in goslings and embryos. We isolated 12 strains of GAstV from 97 positive samples of GAstV prevalent in Sichuan from 2019 to 2022, and determined the GAstV genome copies and virulence of each strain through absolute quantitative methods and subsequent gosling infection experiments, respectively. The results indicated that GAstV SCG3 has the highest virus copies that reaches $1\times10^{9.5}$(Xu et

Received January 3, 2024.
Accepted February 20, 2024.

[1]Corresponding author: shunchen@sicau.edu.cn

al., 2023a). The exceptionally high mortality of GAstV SCG3 in infection experiments compelled us to isolate, culture, and study the characteristics of this virulent strain of GAstV.

GAstV is a small, round, nonenveloped, single-stranded, positive-sense RNA avian astrovirus (Zhang et al., 2017; Chen et al., 2020b). Under a transmission electron microscope, the size of GAstV virions ranges from 28 to 30 nm, and there are typically 5 or 6 star-like protrusions on its surface (Wang et al., 2020; Zhang, et al., 2022c). The genome size of a typical GAstV is approximately 7200 base pairs (**bp**) (Shen, et al., 2022). and the genome consists of 2 noncoding regions (**5′ UTR** and **3′ UTR**), along with 3 open reading frames (**ORF1a, ORF1b, ORF2**) (Yuan, et al., 2019). Among them, ORF1a and ORF1b encode nonstructural proteins, respectively. While ORF2 encodes structural proteins, known as the Cap protein, which is crucial for the formation of infectious particles (Xu et al., 2019; Yin et al., 2021; Wang et al., 2022b). The International Committee on Taxonomy of Viruses classifies GAstV into 2 genotypes: GAstV genotype-1 and GAstV genotype-2 (Zhu and Sun, 2022). There are already multiple methods for quickly detecting and distinguishing different genotypes of goose astroviruses (Yuan et al., 2018; Wan et al., 2019; He et al., 2020; Ji et al., 2020). There are substantial differences in genome sequences between the 2 genotypes, which may be a key factor in the different pathological characteristics of different strains. It has been reported that the GAstV is capable of crossing host barriers and spreading to Beijing ducks, Cherry Valley ducklings and Moscow ducks (Liao et al., 2015; Chen et al., 2020a; Chen et al., 2021), and there are precedents indicating that duck-origin GAstV belongs to the GAstV genotype-2 (Wei et al., 2020b). However, due to the unsuccessful attempts from a large number of infection experiments, it is currently challenging to determine whether different strains of GAstV can lead to varying mortality in goslings and goose embryos.

In this study, we sequenced the genome of the virulent GAstV strain responsible for atypical mortality and established evolutionary trees based on its three main open reading frames to analyze its homology and classify the strain. At the same time, we developed a RT-qPCR method to identify susceptible cells infected with GAstV, and we analyzed the in vitro and in vivo growth kinetics and host specificity of the GAstV strain by measuring the viral load changes during the infection. We also assessed the changes in the genes encoding antiviral cytokines and proteins in LMH cells during GAstV infection to analyze their innate antiviral immune response. In addition, H&E and IHC were performed to determine the GAstV SCG3 viral antigen distribution in the organs and tissues of dead goslings. The characteristics in vitro and in vivo of the atypical virulent GAstV can assist us in further elucidating the pathogenesis of the virulent GAstV strain and the underlying causes for such a high mortality.

MATERIALS AND METHODS

Cells, Viruses, and Antibodies

Cells include LMH, DEF, HEK-293T, Vero, BHK-21, HD-11, DF-1, GEF. Select specific culture medium based on the cultured conditions of various cells. LMH cells were maintained in Dulbecco's modified Eagle's medium Nutrient Mixture F-12 (**DMEM-F12**) (Gibco Shanghai, China) supplemented with 10% fetal bovine serum (**FBS**) (Gibco New York). DEF, BHK-21, HD-11, DF-1, GEF cells were maintained in Dulbecco's modified Eagle's medium (**DMEM**) (Gibco) supplemented with 10% FBS (Gibco). HEK-293T, Vero cells were maintained in Roswell Park Memorial Institute medium 1640 (**RPMI-1640**) (Gibco) supplemented with 10% FBS (Gibco). All cells were incubated at 37℃ with 5% CO_2. GAstV strain SCG2 (GenBank: No. OR234611 and No. OR234619) was isolated from a dead gosling in another farm of the Guanghan district, Deyang City, Sichuan Province on May 8, 2022. GAstV strain SCG3 (GenBank: OQ909424) was isolated from a dead gosling in a farm of the Guanghan district, Deyang City, Sichuan Province on May 9, 2022. The virus stock was grown in goose embryos, and passage 3 was used for the current study. Virus titers in the allantoic fluids, with detection limit of $10^2 TCID_{50}$/mL. The monoclonal antibody against the Cap protein of GAstV was gifted by Professor Zongyan Chen of the Shanghai Veterinary Research Institute.

Embryos and Goslings

A 10-day-old goose embryos were obtained from an independent isolated farm in Hebei province. Ten-day-old duck embryos were obtained from the Ya'an Animal Breeding Base of Sichuan Agricultural University. Three-day-old Tianfu meat goslings were purchased from the Ya'an Animal Breeding Base of Sichuan Agricultural University.

Construction of Standard Curve for Goose Astrovirus

Viral cDNA fragments were synthesized by extracting of GAstV RNA according to the Trizol (Takara, Dalian, China) extraction method. After gel electrophoresis, the kit was used to recover DNA fragments (primers were designed based on ORF1b conserved sequences). These target fragments were then ligated to the PCAGGS vector, transformed, and screened for positive clones. The constructed plasmid was extracted and stored at −20°C. The constructed plasmid was named as pGAstV-ORF1b. The concentration of the pGAstV-ORF1b was measured, and the genome copies were calculated using the provided formula. The absolute quantification of the GAstV ORF1b genome copies were interpolated using a standard curve with 10^8-10^1 copies/μL 10-fold serial dilutions of the pGAstV-ORF1b.

RNA Extraction and RT-qPCR

Total RNA was isolated from cell lysates, allantoic fluids and tissue homogenates by Trizol (Takara, Dalian, China) extraction method. RT-qPCR was carried out in Bio-Rad (Hurcules, CA). For detection of viral RNA from infections, cDNA was first generated using HiScript QRT SuperMix (Vazyme) for RT-PCR according to manufacture' s instructions, and subsequently, qPCR was conducted using 2×Taq SYBR-Green qPCR mix (Innovagene, Changsha, China). The GAstV ORF1b copies were normalized to the total RNA input and report as RNA genome copies per microgram total RNA. For quantification of viral load in infected tissues and allantoic fluids, the viral load was reported as absolute genome copies per μL of viral fluids (L.O.D $1\times10^{0.9}$ GAstV copies/μL) computed based on the standard curve generated from the product of GAstV ORF1b gene. Set up the qPCR reaction system as follows: 2×Taq SYBR Green qPCR Mix 5 mM, Forward Primer 200 μM, Reverse Primer 200 μM, Template DNA 400 μM, and Nuclease-free H_2O 4.2 mM. Initial activation and pre-denaturation at 94℃ for 3 min, followed by 40 cycles of 94℃ 10 s, 55℃ 30 s, and 72℃ 20 s. The antiviral cytokines and proteins were quantitated using the Livak and Schmittgen $2^{-\Delta\Delta CT}$ method and normalized to chicken β-actin, and reported as relative viral RNA expression per microgram total RNA (L.O.D $1\times10^{0.9}$ genome copies/mg). The RT-qPCR primers of measuring GAstV genome copies used in the study were in Table 1 and RT-qPCR primers of measuring chicken cytokines are all in Table 3.

Growth Curve of Goose Astrovirus SCG3

The GAstV SCG3 growth curve was measured by using the cell culture infection dose method in LMH cells. LMH cells were seeded in six 6-well plates, and incubate for 16 h (90% confluence). On each plate, 3 wells were inoculated with 2×10^4TCID$_{50}$ GAstV SCG3, and the other 3 wells served as the mock group. Viral RNAs were collected with at 6 time point: 12 h, 24 h, 36 h, 48 h, 60 h, and 72 h post infection. RT-qPCR was performed to determine the genome copies at each time point to generate the virus growth curve. The curves were obtained by inoculating 2×10^4TCID$_{50}$ and 2×10^5TCID$_{50}$ respectively.

Indirect Immunofluorescence (IFA)

Cells were washed twice with PBS, fixed them with 4% paraformaldehyde for 30 min, and then permeabilized for 30 min at 4°C with 0.3% Triton in PBS. After 1 h of incubation at 37°C with 5% bull serum albumin (**BSA**) in PBS, the cells were treated with mouse anti-GAstV monoclonal antibody (1:500 diluted in PBS containing 1% BSA) for 2 h and then incubated with goat anti-mouse IgG conjugated with FITC (Thermo Fisher Scientific, Shanghai, China; catalog #A16067; 1:1,000 dilution) for 1 h. The cells were then stained with DAPI (Coolaber, Beijing, China) in PBS for 10 min. Each step was followed by three 5 min washes with ice-cold PBST (1‰ Tween-20 in PBS) in an orbital shaker. Fluorescence images were acquired under a fluorescence microscope (Nikon, Tokyo, Japan).

Virulence of Goose Astrovirus SCG3 in Embryos

We measured GAstV genome copies by RT-qPCR in order to determine the infection situation of embryos. Each goose embryo and duck embryo are infected with 2×10^4 TCID$_{50}$ GAstV SCG3. Dead embryos are checked daily post infection with GAstV SCG3. If the embryos died, we would collect their allantoic fluids for RT-PCR and RT-qPCR immediately or place them in a −80℃ refrigerator. RT-PCR and RT-qPCR are used for identification and quantification. After measuring and recording the viral load, continue GAstV SCG3 passage cultivation through embryo inoculation, and the viral load of the allantoic fluids in each generation were

Table 1. Primers used for RT-PCR or RT-qPCR amplification and sequencing of GAstV SCG3.

Primer name	Sequence (5'→3')	Location in genome	Product size (bp)
RT-PCR-GAstV-F1	GCGGCCGGTGGCCCCGCCAGCA	22−43	1464
RT-PCR-GAstV-R1	AAAATGTTCTTCTTATTCTC	3002−2983	
RT-PCR-GAstV-F2	CAGATTTTATTATTCTGTGTT	1465−1485	1518
RT-PCR-GAstV-F3	GAGAATAAGAAGAACATTTT	2983-3002	1815
RT-PCR-GAstV-F4	TCTGGGGTAAATTGGTTTC	4654−4672	844
RT-PCR-GAstV-R4	TCACGTAAATGACAAAAGTT	5497−5478	
RT-PCR-GAstV-F5	AGTGCATTTACTGTTTTCAA	5478−5497	1500
RT-PCR-GAstV-R5	TCGGCGTGGCCGCGGCTGCT	6977−6958	
RT-PCR-GAstV-F6	TGGTGGTGTTTTCTCAAAAATGA	3807−3829	788
RT-PCR-GAstV-R6	ACATTGGGAACTCCAACAAA	4594−4575	
RT-PCR-GAstV-F7	ATGGCGGCCGGTGGCCCCGC	19−38	1467
RT-PCR-GAstV-R7	GGGCCAATTCTCCCTCAAGCCT	7032−7011	1555
PCAGGS-GAstV-ORF1b-F	CATCATTTTGGCAAAGAATTCGCCACCATGG GCAGGATGATATTATTGAGTG	3337−3358	4880
PCAGGS-GAstV-ORF1b-R	TTGGCAGAGGGAAAAAGATCTCTA GGAGCATATTCATCTTGTTG	3496−3466	
RT-qPCR-GAstV-F	GGCAGGATGATATTATTGAGTG	3337−3358	160
RT-qPCR-GAstV-R	GGAGCATATTCATCTTGTTG	3496−3466	

measured to evaluate the efficiency of the in vivo isolation system of GAstV SCG3.

Animal Infection Experiments

We determined the infection status of goslings in order to determine the mortality of goslings infected with GAstV SCG3, viral load and body weight changes. Three-day- old goslings were inoculated via intramuscular injection of 5×10^4 $TCID_{50}$ GAstV SCG3 and same volume of PBS were injected with the control group. Dead goslings were collected daily for organ tissue samples, including heart, liver, spleen, kidney, intestine, and brain postinfection. Part of the samples were used to measure GAstV genome copies, while the other samples were immersed in 10% neutral formalin fixed solution for H&E as well as immunohistochemistry experiments. The goslings would be euthanized if they did not eat or drink any more postinfection with GAstV SCG3. Similarly, tissue samples were taken for GAstV genome copies measurement. Mortality and weight changes of each gosling postinfection with GAstV SCG3 were recorded for 7 d.

Histology and Immunohistochemical Staining

A portion of the spleen, liver, heart, brain, kidney and intestine samples was fixed in buffered 10% formalin for 24 h, dehydrated in graded alcohol, embedded in paraffin wax and cut into 5-μm-thick sections. Some sections were stained with haematoxylin and eosin (**H&E**) using a conventional protocol. Concurrently, slightly modified immunohistochemical (**IHC**) staining was performed. Briefly, a mouse monoclonal antibody against GAstV Cap protein was diluted at 1:500. After an overnight incubation with the primary antibody at 4°C and 3 washes with PBST, the sections were incubated with the goat antimouse secondary antibody (Biotin-Streptavidin HRP Detection Systems, ZSGB-BIO, Beijing, China) for 30 min at 37°C. Finally, the sections were observed under an optical microscope (Nikon, Tokyo, Japan).

Viral Titers Detection

Viral titers were determined by the median tissue culture infectious dose 50 (**$TCID_{50}$**) method in LMH cells. Viral samples were serially diluted 10-fold in DMEM, and then 100 μL dilutions of the viral sample were distributed to each of 8 wells of a 96-well plate seeded with a monolayer of LMH cells. After 120 h incubation at 37°C with 5% CO_2, the presence of viruses was detected by assaying CPE using microscopy, and the viral titers were calculated according to the Reed-Muench method.

Quantification and Statistical Analysis

Data of the RT-qPCR is presented as means ± Standard Error (**SEM**). Student's t test was used to assess statistical significance, with significance defined by P value <0.05 (*) in GraphPad Prism 9.0 software. Statistical significance of survival was analyzed using survival curve, Log-rank (Mantel-Cox) test in GraphPad Prism 9.0 software.

RESULTS

GAstV SCG3 Belongs to Goose Astrovirus Genotype-2 Showing High Homology with AHAU5

Seven pairs of primers were designed for sequencing GAstV SCG3 (Table 1), obtaining the partial genome sequence of GAstV SCG3 including ORF1a, ORF1b and ORF2. Sequence alignments were performed on GAstV SCG3, along with 4 representative strains of GAstV genotype-1 and 4 representative strains of GAstV genotype-2, 5 species of astrovirus, and other 5 waterfowl viruses by using DNAMAN software. Table 2 sequence alignments of ORF1a revealed that it has the closest homologous relationship with AHAU5, JX01, G548 (Figure 1A). Sequence alignments of ORF1b indicated that it has the closest homology with AHAU5, G548, JX01 (Figure 1B). Sequence alignments of ORF2 revealed that it has the closest homology with G548, AHAU5, JX01 (Figure 1C). Overall, it was found that GAstV AHAU5 exhibits the closest homology with GAstV SCG3.

GAstV SCG3 Can Cross Host to Infect LMH Cells In Vitro Due to Its Liver Targeting

The allantoic virus can be subcultured in both goose embryos and duck embryos for 5 generations postinfection with GAstV SCG3, while only subculturing by goose embryos is the efficient way to cultivate GAstV SCG3. GAstV SCG3 does not induce cytopathic effects in cell lines including DEF, GEF, HEK-293T, Vero, BHK-21, HD-11, DF-1, which is known as the self-limiting of GAstV replication, while GAstV SCG3 can lead to severe cytopathic effects in LMH cells (Figure 2A). Based on the results of the IFA experiments, where LMH cells were infected with GAstV SCG3, it can be observed that the green fluorescence generated by GAstV SCG3 is surrounded by the blue fluorescence from the nucleus. This indicates that GAstV SCG3 can infect LMH cells. However, GAstV SCG3 cannot enter the nucleus and primarily relies on LMH cells to replicate in the cytoplasm outside the nucleus (Figure 2B). We performed absolute quantification of the viral load by establishing an RT-qPCR standard curve for GAstV. In vitro GAstV culture experiments were conducted, and the results demonstrated that only LMH cells were capable of stably cultivating GAstV SCG3 for up to 10

Table 2. Alignments with the nucleotide identities of GAstV SCG3.

Astrovirus (GenBank accession no.)	Percent identify (%) to Goose astrovirus SCG3(OQ909424)			
	Genome(bp)	ORF1a(aa)	ORF1b(aa)	ORF2(aa)
Goose astrovirus GD (MG934571.1)	7183	97.34	98.08	96.84
Goose astrovirus JX01(MZ576222.1)	7173	97.98	98.28	97.83
Goose astrovirus AHAU5(MN428645.1)	7182	99.26	99.30	97.79
Goose astrovirus G548(OM273309.1)	7183	97.46	98.65	98.87
Goose astrovirus SCCD(MW786757.1)	7255	52.52	60.84	48.46
Goose astrovirus AHDY(MH410610.1)	7288	52.80	60.78	48.12
Goose astrovirus ZJC14 (MZ819185.1)	7288	52.61	60.46	48.19
Goose astrovirus FLX (NC_034567.1)	7299	52.43	60.56	47.59
Turkey astrovirus (NC_002470.1)	7003	23.26	5.96	15.02
Feline astrovirus (NC_024701.1)	6598	20.16	12.14	14.28
Human astrovirus (NC_001943)	6813	19.64	11.80	13.31
Pig astrovirus (MT470220.1)	6721	20.12	11.86	12.85
Chicken astrovirus (MZ367372)	7480	24.2	13.31	13.40
Duck astrovirus (OM095382.1)	7517	24.27	13.30	14.44
Adenovirus (J01917.1)	35937	3.79	1.76	2.40
Tembusu virus (KF192951.1)	10989	12.19	5.96	8.49
Goose paramyxovirus (NC_005036.1)	15192	9.09	4.41	5.77
Goose parvovirus (KC996730.1)	5046	4.96	10.96	6.90
Influenza A virus (JN852792.1)	2191	27.38	29.43	39.19

generations. Furthermore, GAstV SCG3 maintained a consistently high viral load in each generation (Figure 3A−3K). The stable passage culture can aid in establishing the growth curve of GAstV SCG3 and providing insights into the characteristics of GAstV SCG3 in vitro.

GAstV SCG3 Can Activate Antiviral Response in LMH Cells During the Infection

We evaluated the host's antiviral response to viral infection in the presence of GAstV SCG3. We confirmed that GAstV SCG3 can trigger antiviral response of the host cells. Compared to the control infected cells, IL-1β, NF-κB, IFN-α, IFN-β, OASL and Mx exhibited the most significant increase 24 h postinfection with GAstV SCG3. This observation may be closely associated with the high virulence of GAstV SCG3. However, there was a substantial decrease in IL-1β, NF-κB, IFN-α, IFN-β, OASL and Mx 48 h postinfection with GAstV SCG3 (Figure 4A−4F). By 72 h, these antiviral cytokines had already reached a relatively low level, which can be attributed to the high viral load observed at this time. These changes align with the alterations in viral load, and the reason that GAstV failed to proliferate in LMH cells unlimitedly may also be associated with the presence of a certain level of antiviral response 72 h postinfection with GAstV SCG3. The decrease in the level of antiviral response may be linked to the extensive cell death induced by GAstV proliferation during the infection process. RT-qPCR primers employed for measuring chicken cytokines can be found in Table 3.

GAstV SCG3 Has High Pathogenicity and Host Specificity In Vivo Infection

We observed the infection status of goslings, goose embryos and duck embryos 7 d postinfection with

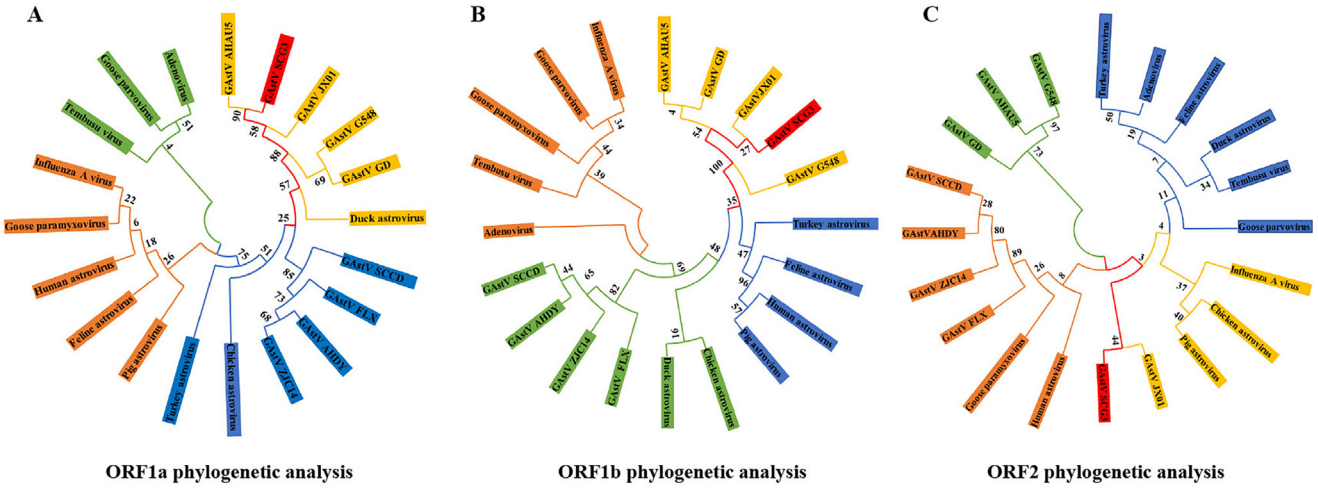

Figure 1. Phylogenetic analysis of GAstV SCG3 open reading frames. (A) Phylogenetic tree of GAstV SCG3 ORF1b. (B) Phylogenetic tree of GAstV SCG3 ORF1b. (C) Phylogenetic tree of GAstV SCG3 ORF2. The trees were generated using MEGA 7.0 software and the Neighbor-joining method with 1000 bootstrap replicates.

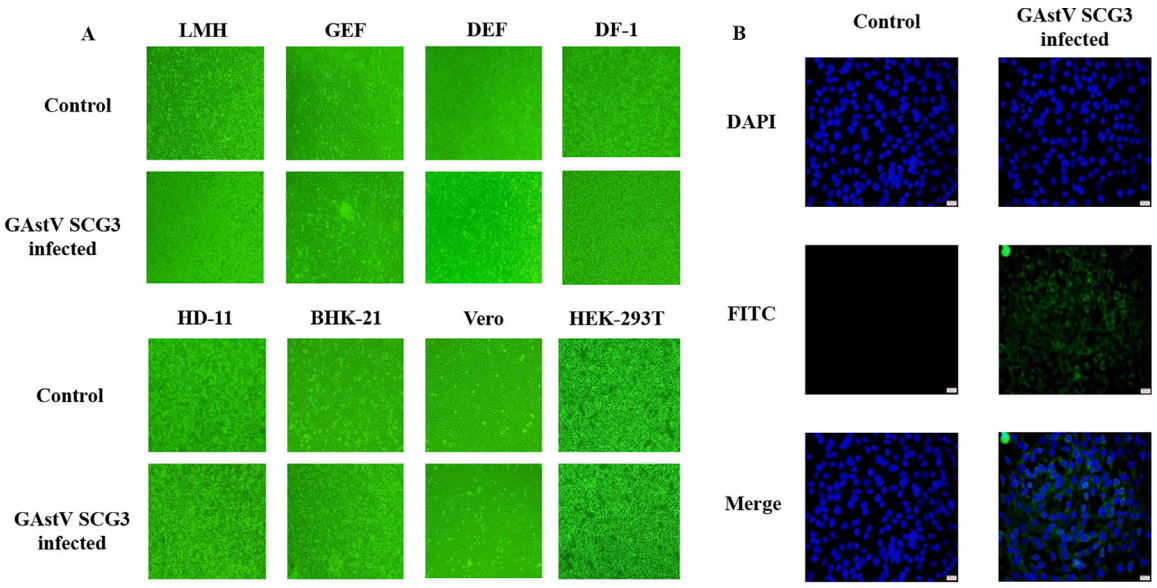

Figure 2. Cell culture characteristics of GAstV SCG3. (A) Cell pathological changes of different cells (LMH, GEF, DEF, DF-1, HD-11, BHK-21, Vero, HEK-293T) 3 d postinfection (dpi). The infective dose of all cells is 2×10^4 $TCID_{50}$ GAstV SCG3. Equal volume of PBS was used as the control group. (B) GAstV SCG3-infected LMH cells stained for GAstV antigen (green) and nuclei (blue) on 2 d postinfection (dpi). Mock infected cells were used as controls. The images were recorded using an OLYMPUS upright fluorescence microscope. The nuclei were stained with DAPI (blue) and the antigens were stained with FITC (green). Scale bar, 20 μm.

GAstV SCG3 (Figure 5A), it was found that the mortality of goslings and goose embryos can be as high as 93 and 80%, respectively. While the mortality among duck embryos was observed to be 0 (Figure 5B), indicating that the GAstV strain is virulent and host specific. Goslings infected with GAstV SCG3 exhibit gray discoloration of the eyelids, and difficulty in standing, and their growth was significantly inhibited (Figure 5C). GAstV SCG3 demonstrates strong virulence in goslings and goose embryos with a survival rate of only 6.2% among goslings, leading to their demise within 2 d postinfection (Figure 5D). Surprisingly, on the third day of GAstV SCG3 infection experiment, 12 goslings succumbed the same day (Figure 5E). Dissecting dead goslings infected

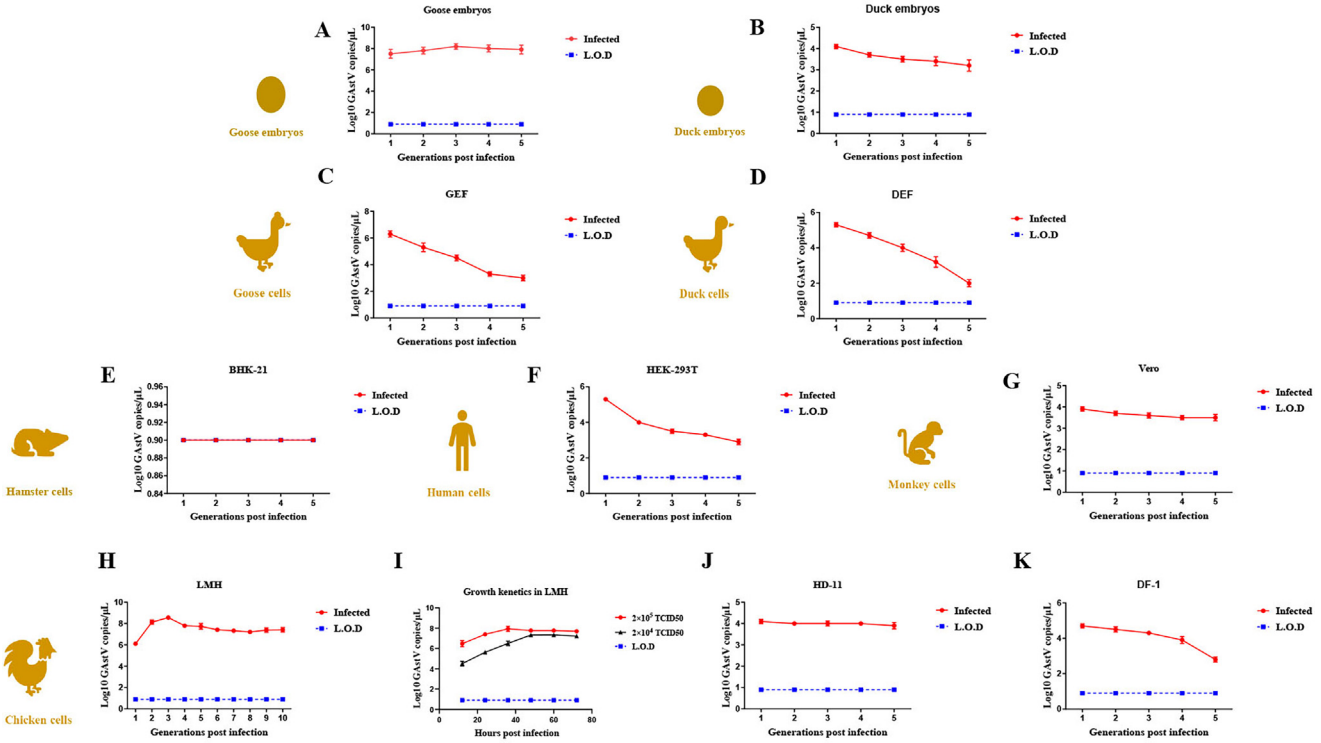

Figure 3. Growth kinetics of GAstV in vitro. For (A)goose embryos, (B) duck embryos, (C) GEF cells, (D) DEF cells, (E) BHK-21 cells, (F) HEK-293T cells, (G) Vero cells, (H) LMH cells, (J) HD-11 cells and (K) DF-1 cells, the infective dose of all cells is 2×10^4 $TCID_{50}$ GAstV SCG3. (I) Growth curve of GAstV SCG3 in LMH cells. The infective doses used in growth curve are 2×10^4 $TCID_{50}$ GAstV SCG3 and 2×10^5 TCID50 GAstV SCG3, respectively. Equal volume of PBS was used as the control group. The limit of detection (L.O.D) of RT-qPCR is $1\times10^{0.9}$ GAstV copies/μL.

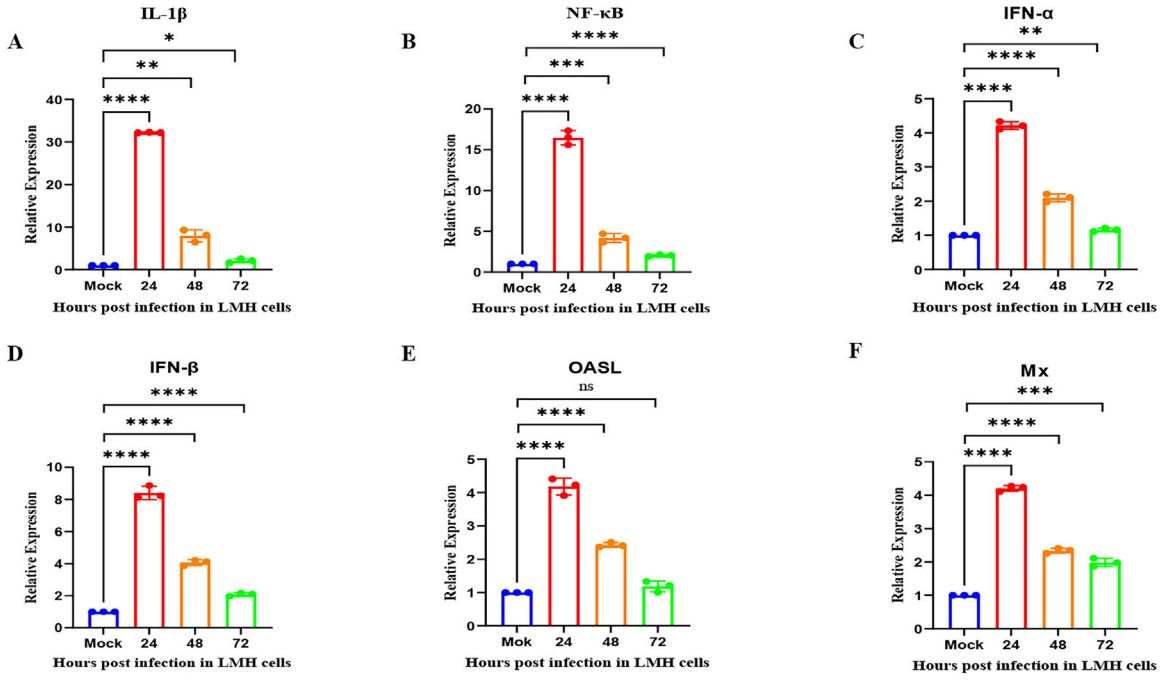

Figure 4. Relative expression levels of cytokines induced by GAstV SCG3 by RT-qPCR. The infective dose of LMH cells is 5×10^4 $TCID_{50}$ GAstV SCG3. Equal volume of PBS was used as the control group. (A) IL-1β. (B) NF-κB. (C) IFN-α. (D) IFN-β. (E) OASL. (F)Mx. The y-axis represents the relative expression level. The relative expression of all genes was calculated using the Livak and Schmittgen $2^{-\Delta\Delta CT}$ method and normalized to chicken β-actin. The limit of detection (L.O.D) of RT-qPCR is $1\times10^{0.9}$ genome copies/μL. Data are represented as the means ± SD (n = 6). * indicates statistically significant differences. (ns indicates not significant, * indicates $P \leq 0.05$, ** indicates $P \leq 0.01$, *** indicates $P \leq 0.001$.**** indicates $P \leq 0.0001$).

with GAstV SCG3 can reveal atypical mortality in their intestines, as well as severe congestion in organs such as the liver, kidney, and spleen in contrast to tissues infected with attenuated strain GAstV SCG2 (Figure 5F). When goslings and duck embryos were infected with GAstV SCG3, it was observed that the survival rate of goose embryos reached 20% (Figure 5G), 1 potential reason why the same dose of GAstV SCG3 may result in varying mortality rates in goose embryos is the number embryos used in this experiment, the last experiment n = 3, but this time n = 10. It's also need to aware that different goose embryos were collected from goose breeding farm which may be very individual (no SPF goose embryos is available). However, both of those 2 results confirmed that this strain (GAstV SCG3) is virulent and exhibits a high mortality in goose embryos. the mortality among duck embryos remained at 0 (Figure 5H). The embryo membrane would become thicker and the bleeding points would increase postinfection of goose embryos with GAstV SCG3 (Figure 5I). After removing the embryo shell, it became apparent that the embryo exhibited mortality, and the liver lost its natural color and experienced tissue degeneration in contrast to tissues infected with attenuated strain GAstV SCG2 (Figure 5J). Different from the attenuated strain SCG2, measurement about the viral load of dead gosling tissues postinfection with GAstV SCG3 indicated that the liver had the highest viral load, followed by the kidney, spleen, intestine, heart, and brain (Figure 6A−6F)

Table 3. RT-qPCR primers of measuring chicken cytokines.

Primer name	GenBank accession no.	Location in genome	Sequence (5′→3′)
RT-qPCR-Chicken IFN-α-F	DQ226092.1	334−353	CGCCAAAGCCTCCTCAACCG
RT-qPCR-Chicken IFN-α-R		507−488	GGCGCAGGCGCTGTAATCGT
RT-qPCR-Chicken IFN-β-F	NM_001024836.2	96−115	TCACCAGGATGCCAACTTCT
RT-qPCR-Chicken IFN-β-R		321−302	TGTGCGGTCAATCCAGTGTT
RT-qPCR-Chicken OASL-F	NM_001397447.1	646−665	CGCCTGGTCAAGCACTGGTA
RT-qPCR-Chicken OASL-R		885−865	GTAGGCACCGACCCACTCATC
RT-qPCR-Chicken Mx-F	NM_204609.2	163−182	CAATCCACGGTCCAACTTCA
RT-qPCR-Chicken Mx-R		398−377	CTGCCTCATCCTTGTCCTCTTC
RT-qPCR-Chicken IL-1β-F	NM_204524.2	267−286	GACCAAACTGCTGCGGAGGC
RT-qPCR-Chicken IL-1β-R		421−401	CGAAGGACTGTGAGCGGGTGT
RT-qPCR-Chicken NF-κB-F	BG625630.1	128−147	GCTCACAAAGGCAGTCTCAC
RT-qPCR-Chicken NF-κB-R		345−326	CTTGCTAAGCGTTATGGATG
RT-qPCR-Chicken β-actin-F	L08165.1	1179−1198	CACCGCAAATGCTTCTAAAC
RT-qPCR-Chicken β-actin-R		1352−1333	AAGACTGCTGCTGACACCTT

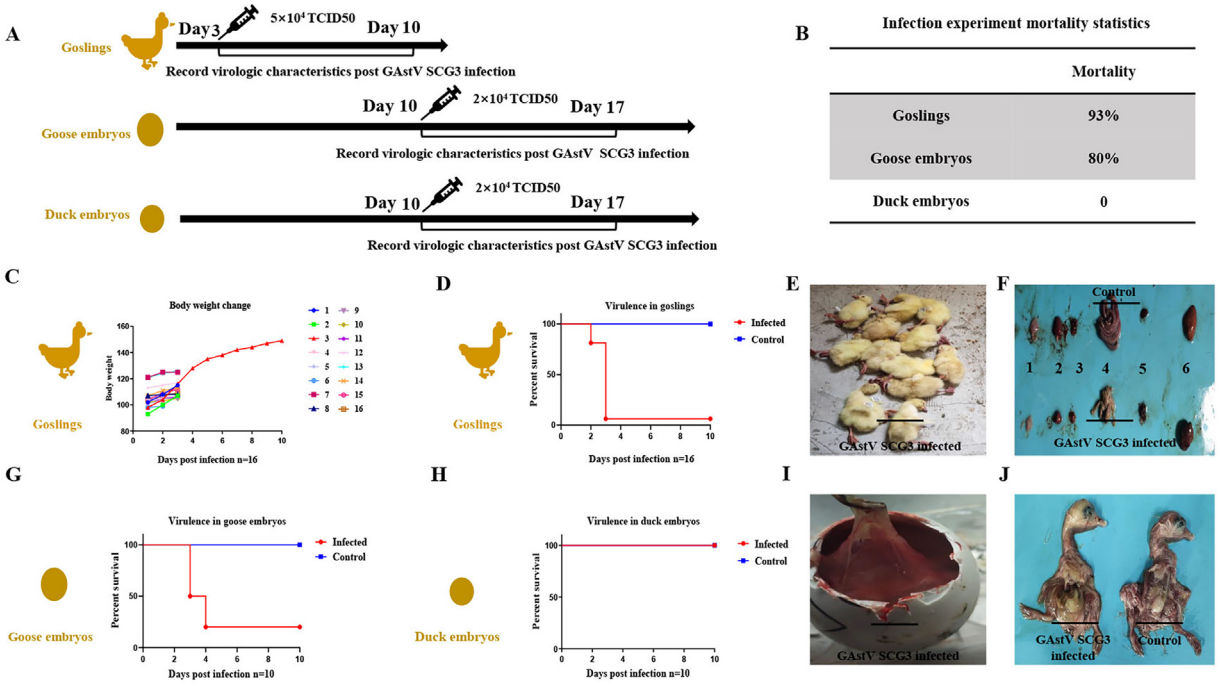

Figure 5. GAstV SCG3-infected animal experiment. The infective dose of all goslings is 5×10^4 $TCID_{50}$ GAstV SCG3, Equal volume of PBS was used as the control group. (A) Operating procedure of animal infection experiments. (B) Results of animal infection experiments. (C) Body weight changes of gosling postinfection with GAstV SCG3. (D) Survival percent of goslings postinfection with GAstV SCG3. (E) A large number of goslings died at once 3 d postinfection with GAstV SCG3. (F) Anatomy diagrams of dead group infected with GAstV SCG3 and an equal volume of PBS were used as the control group. 1−6: brain, heart, spleen, intestine, kidney, liver. (G) Survival percent of goose embryos postinfection with GAstV SCG3. (H) Survival percent of duck embryos postinfection with GAstV SCG3. (I) Fetal membranes of goose embryos thickened 3 d postinfection with GAstV SCG3. (J) Embryos anatomy diagrams of dead group infected with GAstV SCG3 and equal volume of PBS was used as the control group.

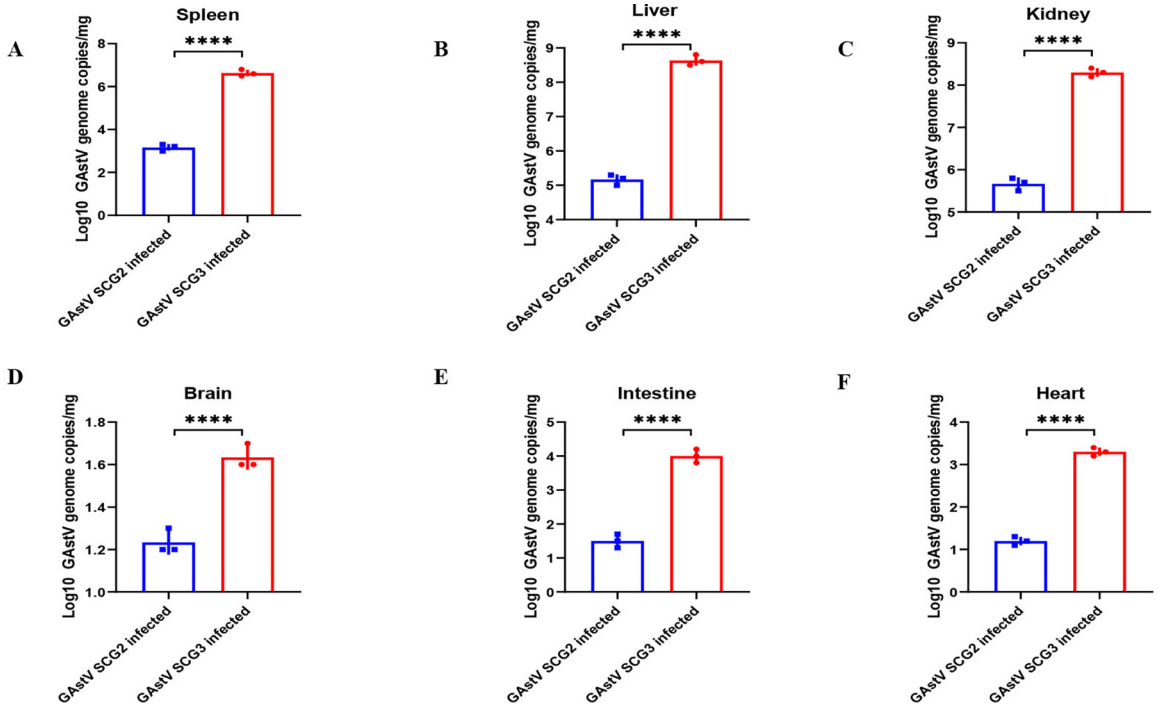

Figure 6. Tissues virus loads of GAstV in the infected goslings. (A) Spleen. (B) Liver. (C) Kidney. (D) Brain. (E) Intestine. (F) Heart. The infective dose of all goslings is 5×10^4 $TCID_{50}$ GAstV SCG3. Equal volume of PBS was used as the control group. All Ct values are measured by established qPCR method and converted from standard curves to GAstV genome copies. Values shown as means ± SD from a minimum of 3 biological replicates. A one-way ANOVA was performed unless otherwise indicated. Throughout this study, * indicates statistically significant differences. Results are shown as means ± SD (n = 6). Unpaired t-test shows that difference is $^{****}P \leq 0.0001$.

GAstV SCG3 Has Extensive Tissue Phagocytosis in Target Organs

The dead goslings exhibited clinical signs of severe tissue damage, indicating pathological changes in the tissues. Therefore, further analyses were conducted on selected tissues such as the spleen, liver, heart, brain, kidney, and intestine. In the spleen tissues, a substantial amount of white pulp was observed, with a decrease in the number and structure, and a lack of obvious white pulp. The boundary between white pulp and red pulp was unclear, along with extensive congestion (indicated by black arrows), scattered lymphocyte necrosis, karyorrhexis (indicated by blue arrows), and some neutrophil infiltration (indicated by green arrows) (Figure 7A). In the liver tissue, diffuse hepatocyte steatosis was evident, with round vacuoles of varying sizes observed in the cytoplasm (indicated by black arrows). Severe congestion and dilation of large hepatic sinuses were also present (indicated by blue arrows), along with excessive central venous congestion (indicated by green arrows) (Figure 7B). Calcifications were visible in the epicardium of the heart tissue (indicated by black arrows), along with connective tissue hyperplasia and a small number of lymphocytes (indicated by blue arrows) (Figure 7C). The brain did not exhibit significant lesions (Fig. 7D). In the kidney tissue, a small amount of watery degeneration of renal tubular epithelial cells was noticeable, characterized by loose and lightly stained cytoplasm (indicated by black arrows). There was also extensive renal tubulointerstitial congestion and dilation (indicated by blue arrows), along with excessive vascular congestion and dilation (indicated by green arrows) (Figure 7E). In the intestinal tissue, a significant number of intestinal villi were observed to have shortened, with some intestinal villi showing necrosis, structure disappearance, and the necrotic shedding of a large number of mucosal epithelial cells (indicated by black arrows). The lamina propria was exposed, revealing numerous intestinal glands with incomplete structure and a substantial amount of epithelial shedding (indicated by green arrows), and there was also a minor infiltration of lymphocytes in the submucosa (indicated by yellow arrows) (Figure 7F) (Ding et al., 2021; Huang et al., 2021). All of these results indicate that GAstV SCG3 can lead to varying degrees of damage to the heart, liver, spleen, and intestines, with the liver being the most severely affected organ. Severe tissue phagocytosis in the liver results in serious disorders of metabolic enzymes.

GAstV SCG3 Enriched in Target Organs Causes Severe Damage Inducing Fatal Gout

Through immunohistochemistry experiments, it was observed that the liver had the strongest positive signal, suggesting that the antigen of GAstV SCG3 is primarily distributed in the liver, followed by kidney, spleen, intestine, heart and brain. In comparison to the attenuated strain GAstV SCG2, GAstV SCG3 demonstrates efficient proliferation in its main target organs, while the attenuated strain struggles to cause mortality in goslings. Furthermore, the GAstV SCG2 genome copies in its tissues are significantly lower than those of GAstV SCG3. The highest GAstV SCG2 genome copies in its tissues were found in the kidney, followed by the liver, spleen, intestine, heart, and intestine. This observation aligns with previously reported results, and the distribution of GAstV virons in tissues is consistent with the outcomes of nephrotic astrovirus infections (Yuan et al.,

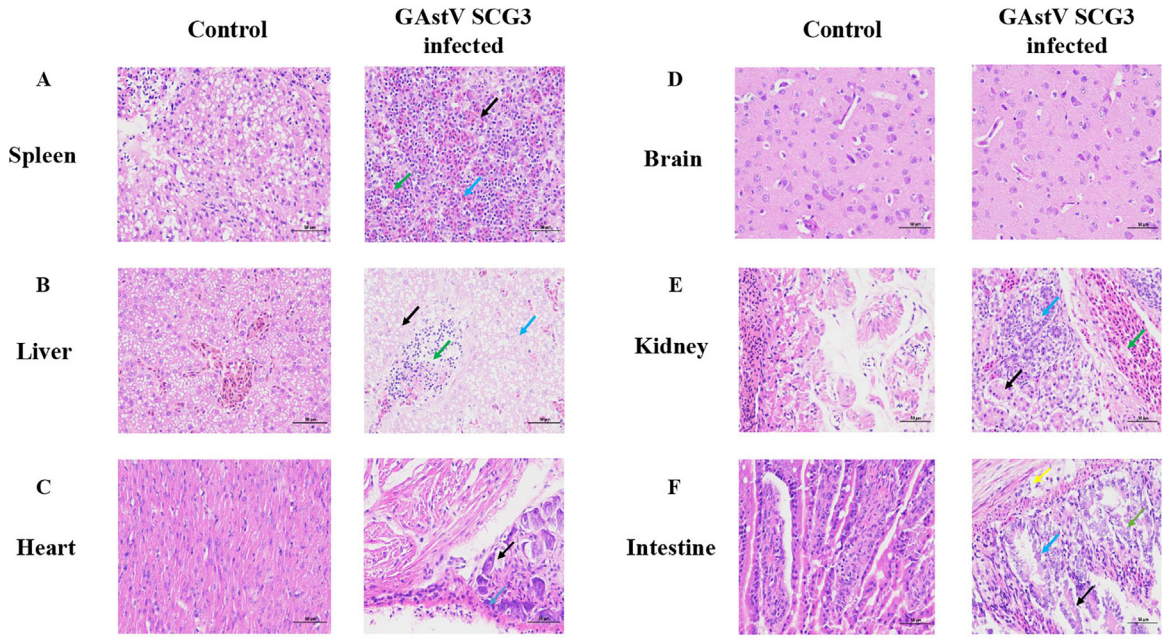

Figure 7. Representative hematoxylin and eosin staining of infected and control tissues. Histological changes in the tissues from dead gosling post infection with 5×10^4 $TCID_{50}$ GAstV SCG3. Equal volume of PBS was used as the control group. (A) spleen, (B) liver, (C) heart, (D) brain, (E) kidney and (F) intestine. Green arrows, blue arrows, black arrows, yellow arrows indicate different pathological characteristics. Scale bar, 50 μm.

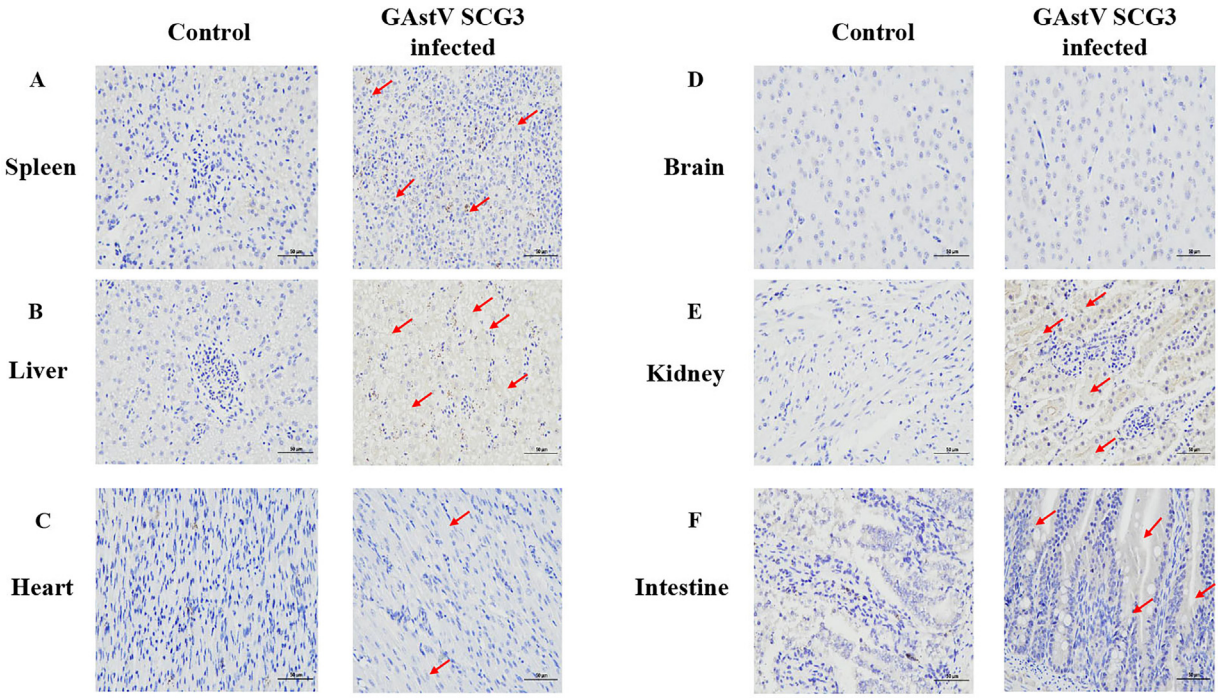

Figure 8. Representative immunohistochemical staining of infected and control tissues. (A) spleen, (B) liver, (C) heart, (D) brain, (E) kidney and (F) intestine. GAstV distribution in the dead gosling tissues post infection with 5×10^4 $TCID_{50}$ GAstV SCG3 evaluated via an IHC analysis. Equal volume of PBS was used as the control group. Red arrows indicate positive signals. Scale bar, 50 μm.

2019). (Figure 8A−8F), while the positive signal in intestine, heart, and brain is very attenuated (indicated by red arrows). This suggests that GAstV SCG3 can effectively replicate in the liver, kidney, and spleen, and the most critical host organ is liver. The liver exhibits the highest positive cell rate, strongly positive in brown-yellow. According to the grading of positive cell rate, the positive rate of liver reaches 44.7%, reaching level 2 (26−50%) indicating that the GAstV antigen is predominantly concentrated in the liver. The extensive invasion of the target organs by a large number of GAstV can result in severe damage, which can be the underlying cause of fatal gosling gout (Guo et al., 2019).

DISCUSSION

The clinical symptoms of GAstV infection include joint swelling and the typical uric acid precipitation in goose visceral organs, with mortality no more than 50% (Xu et al., 2023b). GAstV has inflicted significant damage on the waterfowl industry in recent years (Liu, et al., 2020; Wang et al., 2021; Fu et al., 2022). GAstV has now spread to many provinces of China, including Shandong, Guangdong, Anhui, and Jiangxi et al. (Yang et al., 2018; Wu et al., 2020; Zhang et al., 2022b). The most recent outbreaks of the GAstV account for more than 80% of all goose-origin viruses in Sichuan. Due to the differences in viral proteins encoded by virulence genes of GAstV, GAstV may also induce distinct pathological characteristics (Cui et al., 2022; Fei et al., 2022). However, it is currently unknown which specific virulence gene is the most critical in influencing the virulence of GAstV and determining its host specificity. Due to lack of animal infection experiments involving different strains of GAstV, it is challenging to identify and compare the pathological characteristics of goslings infected with various GAstV strains. The only known fact is that GAstV genotype-2 can lead to severe urate deposition in the organs and joints, resulting in severe gosling gout (Li et al., 2021).

In recent years, gosling gout has been regarded as one of the most important threats impacting the waterfowl industry (Wang et al., 2022a; Zhang et al., 2022b). Apart from factors such as nutrition disorder, food mycotoxins contamination, vitamin deficiency and other feeding and management aspects, GAstV infection is regarded as the primary underlying cause of large-scale gosling gout in farms (Liu et al., 2018; Zhang et al., 2018b). The main causes of gosling gout are excessive uric acid accumulation in the body and impaired uric acid excretion in goslings (Xi et al., 2019; Xi et al., 2022). GAstV primarily inflicts serious damage on the metabolic organs of goslings, resulting in uric acid excretion disorders in goslings, which in turn lead to a significant increase in blood uric acid levels. Large quantities of white urate salts are deposited in organs or joints, forming urate crystals and resulting in gout (Niu, et al., 2018).

GAstV SCG3 in this study has several important atypical characteristics: 1) GAstV SCG3 is virulent with mortality of 93% and 80% in goslings and goose embryos, respectively. 2) GAstV SCG3 has extensive tissue phagocytosis and can cause significant lesions in organs such as the liver, spleen, and kidney. 3) GAstV SCG3 can seriously stun the growth of infected goslings. GAstV SCG3 along with the reported AHAU5, JX01,

G548, belongs to the GAstV genotype-2. However, GAstV SCG3 can cause atypical mortality, which may be caused by multiple mutations in its viral proteins (Ren et al., 2020; Ren et al., 2022). 4) GAstV SCG3 can activate the antiviral innate immune response in LMH cells, and its ability to activate a large number of inflammatory genes at 24 h postinfection may be due to its ability to cause severe and fatal liver injury (Wu et al., 2021). The activation of antiviral cytokines and antiviral proteins of GAstV SCG3 may be the cause of the self-limiting of replication, which may make it difficult for prolonged propagation of the virus in cells. 5) The study on the growth kinetics of GAstV SCG3 in vitro and in vivo indicated that GAstV SCG3 can only be continuously cultured through LMH cells and goose embryos, which means GAstV SCG3 may have specific organ/tissue tropism. 6) GAstV SCG3 can be widely distributed in and damaged the liver, kidney, spleen, intestine, and heart of goslings. Significantly, the liver has significantly higher antigen positive rate than other organs.

Isolating and cultivating GAstV has consistently posed a significant challenge. Our research has unveiled that achieving efficient isolation and cultivation of GAstV SCG3 in vitro is only feasible through the utilization of goose embryos and LMH cells. The results of differences in virulence among different strains of GAstV isolates shows that all GAstV isolates exhibit different adaptations to different hosts and varying degrees of damage to tissues and organs. Overall, the strains with higher viral load have stronger pathogenicity and exhibit higher lethality against waterfowl in vivo infection experiments. We found GAstV SCG3 has extensive tissue phagocytosis, the viral load in the liver of dead gosling is even higher than that in the kidney, and its high pathogenicity to the liver may be the important reason for its ability to cross host infect cells. The virulent strain of GAstV enriched in liver causes fatal liver damages inducing gout. Our study's observation of this phenomenon is a novel and significant contribution that can help further understanding on the pathogenicity of GAstV and the cause of such a high mortality. A comparison between the genome and amino acid sequences of the highly virulent strain revealed the highest homology with AHAU5. These findings serve as crucial references for further exploration of efficient isolation and cultivation ways for GAstV both in vitro and in vivo. Our study provides valuable insights for researchers in this field.

ACKNOWLEDGMENTS

This work was funded by grants from the National Key Research and Development Program of China (2022YFD1801900), National Natural Science Foundation of China (32272976), Sichuan Provincial Department of science and technology international scientific and technological innovation cooperation (2022YFH0026), the earmarked fund for China Agriculture Research System(CARS-42-17), and the Program Sichuan Veterinary Medicine and Drug Innovation Group of China Agricultural Research System (SCCXTD-2021-18).

Ethical Statement: All animal experimental procedures were approved by the Institutional Animal Care and Use Committee of Sichuan Agriculture University in Sichuan, China (Protocol Permit Number: SYXK(川) 2019-187).

Authors Contributions: LX, ZW, YH, BJ, YC, MW, RJ, DZ, ML, XZ, QY, YW, SZ, JH, XO, DS, AC and SC: conceptualization. LX, BJ and SC: methodology. LX and SC: data curation. BJ: formal analysis. AC and SC: funding acquisition and project administration. SC: resources and supervision. LX: writing−original draft. SC, ZW, YH: review & editing. All authors contributed to the article and approved the final manuscript.

Data Availability Statement: The data that support the findings of this study are available from the corresponding author upon reasonable request. The sequences of GAstV SCG2 ORF1b and GAstV SCG2 ORF2 have been submitted to GenBank, under the accession number of No. OR234611 and No. OR234619, respectively. Besides, the sequences of GAstV SCG3 have been submitted to GenBank, under the accession number of OQ909424.

The GAstV genome copies were quantified using RT-qPCR through the standard curve: Y=42.522−3.336 logX, R^2=0.9998, the run efficiency is 99.434% (Y is the Ct value and X is the GAstV genome copies), supplementary materials are in Figure S1.

DISCLOSURES

The authors declare that the research was conducted in the absence of any commercial or financial relationships that could be construed as a potential conflict of interest.

SUPPLEMENTARY MATERIALS

Supplementary material associated with this article can be found in the online version at doi:10.1016/j.psj.2024.103585.

REFERENCES

An, D., J. Zhang, J. Yang, Y. Tang, and Y. Diao. 2020. Novel goose-origin astrovirus infection in geese: the effect of age at infection. Poult. Sci. 99:4323–4333.

Bidin, M., Z. Bidin, D. Majnaric, M. Tisljar, and I. Lojkic. 2012. Circulation and phylogenetic relationship of chicken and turkey-origin astroviruses detected in domestic ducks (*Anas platyrhynchos domesticus*). Avian Pathol. 41:555–562.

Chen, H., B. Zhang, M. Yan, Y. Diao, and Y. Tang. 2020a. First report of a novel goose astrovirus outbreak in Cherry Valley ducklings in China. Transbound. Emerg. Dis. 67:1019–1024.

Chen, Q., X. Xu, Z. Yu, C. Sui, K. Zuo, G. Zhi, J. Ji, L. Yao, Y. Kan, Y. Bi, and Q. Xie. 2020b. Characterization and genomic analysis of emerging astroviruses causing fatal gout in goslings. Transbound. Emerg. Dis. 67:865–876.

Chen, Q., Z. Yu, X. Xu, J. Ji, L. Yao, Y. Kan, Y. Bi, and Q. Xie. 2021. First report of a novel goose astrovirus outbreak in Muscovy ducklings in China. Poult. Sci. 100:101407.

Cui, H., X. Mu, X. Xu, J. Ji, K. Ma, C. Leng, L. Yao, Y. Kan, Y. Bi, and Q. Xie. 2022. Extensive genetic heterogeneity and molecular characteristics of emerging astroviruses causing fatal gout in goslings. Poult. Sci. 101:101888.

Ding, R., H. Huang, H. Wang, Z. Yi, S. Qiu, Y. Lv, and E. Bao. 2021. Goose nephritic astrovirus infection of goslings induces lymphocyte apoptosis, reticular fiber destruction, and CD8 T-Cell depletion in spleen tissue. Viruses. 13:1108.

Fei, Z., A. Jiao, M. Xu, J. Wu, Y. Wang, J. Yu, L. Lu, W. Jiang, G. Zhu, W. Sun, Z. Chen, Y. Zhang, S. Ren, F. Liu, and L. Zhang. 2022. Genetic diversity and evolution of goose astrovirus in the east of China. Transbound. Emerg. Dis. 69:e2059–e2072.

Fu, X., Z. Hou, W. Liu, N. Cao, Y. Liang, B. Li, D. Jiang, W. Li, D. Xu, Y. Tian, and Y. Huang. 2022. Insight into the epidemiology and evolutionary history of novel goose astrovirus-associated gout in goslings in Southern China. Viruses. 14:1306.

Guo, R., L. D. Berry, D. L. Aisner, J. Sheren, T. Boyle, P. A. Bunn Jr., B. E. Johnson, D. J. Kwiatkowski, A. Drilon, L. M. Sholl, and M. G. Kris. 2019. MET IHC is a poor screen for MET amplification or MET Exon 14 mutations in lung adenocarcinomas: data from a tri-institutional cohort of the lung cancer mutation consortium. J. Thorac. Oncol. 14:1666–1671.

He, D., F. Wang, L. Zhao, X. Jiang, S. Zhang, F. Wei, B. Wu, Y. Wang, Y. Diao, and Y. Tang. 2022. Epidemiological investigation of infectious diseases in geese on mainland China during 2018-2021. Transbound. Emerg. Dis. 69:3419–3432.

He, D., J. Yang, X. Jiang, Y. Lin, H. Chen, Y. Tang, and Y. Diao. 2020. A quantitative loop-mediated isothermal amplification assay for detecting a novel goose astrovirus. Poult. Sci. 99:6586–6592.

Huang, H., R. Ding, Z. Chen, Z. Yi, H. Wang, Y. Lv, and E. Bao. 2021. Goose nephritic astrovirus infection increases autophagy, destroys intercellular junctions in renal tubular epithelial cells, and damages podocytes in the kidneys of infected goslings. Vet. Microbiol. 263:109244.

Ji, J., Q. Chen, C. Sui, W. Hu, Z. Yu, Z. Zhang, X. Mu, X. Xu, L. Yao, Y. Kan, and Q. Xie. 2020. Rapid and visual detection of novel astroviruses causing fatal gout in goslings using one-step reverse transcription loop-mediated isothermal amplification. Poult. Sci. 99:4259–4264.

Li, J. Y., W. Q. Hu, T. N. Liu, H. H. Zhang, T. Opriessnig, and C. T. Xiao. 2021. Isolation and evolutionary analyses of gout-associated goose astrovirus causing disease in experimentally infected chickens. Poult. Sci. 100:543–552.

Liao, Q., N. Liu, X. Wang, F. Wang, and D. Zhang. 2015. Genetic characterization of a novel astrovirus in Pekin ducks. Infect. Genet. Evol. 32:60–67.

Liu, H., D. Hu, Y. Zhu, H. Xiong, X. Lv, C. Wei, M. Liu, D. Yin, C. He, K. Qi, and G. Wang. 2020. Coinfection of parvovirus and astrovirus in gout-affected goslings. Transbound. Emerg. Dis. 67:2830–2838.

Liu, M., Y. Zhao, D. Hu, X. Huang, H. Xiong, K. Qi, and H. Liu. 2019. Clinical and histologic characterization of co-infection with astrovirus and goose parvovirus in goslings. Avian Dis. 63:731–736.

Liu, N., M. Jiang, Y. Dong, X. Wang, and D. Zhang. 2018. Genetic characterization of a novel group of avastroviruses in geese. Transbound. Emerg. Dis. 65:927–932.

Niu, X., J. Tian, J. Yang, X. Jiang, H. Wang, H. Chen, T. Yi, and Y. Diao. 2018. Novel goose astrovirus associated gout in Gosling, China. Vet. Microbiol. 220:53–56.

Ren, D., T. Li, W. Zhang, X. Zhang, X. Zhang, Q. Xie, J. Zhang, H. Shao, Z. Wan, A. Qin, J. Ye, and W. Gao. 2022. Identification of three novel B cell epitopes in ORF2 protein of the emerging goose astrovirus and their application. Appl. Microbiol. Biotechnol. 106:855–863.

Ren, D., T. Li, X. Zhang, X. Yao, W. Gao, Q. Xie, J. Zhang, H. Shao, Z. Wan, A. Qin, and J. Ye. 2020. OASL triggered by novel goose astrovirus via ORF2 restricts its replication. J. Virol. 94:e01767-20.

Shen, Q., Z. Zhuang, J. Lu, L. Qian, G. Li, A. G. Kanton, S. Yang, X. Wang, H. Wang, J. Yin, and W. Zhang. 2022. Genome analysis of goose-origin astroviruses causing fatal gout in Shanghai, China reveals one of them belonging to a novel type is a recombinant strain. Front. Vet. Sci. 9:878441.

Wan, C., C. Chen, L. Cheng, G. Fu, S. Shi, R. Liu, H. Chen, Q. Fu, and Y. Huang. 2019. Specific detection of the novel goose astrovirus using a TaqMan real-time RT-PCR technology. Microb. Pathog. 137:103766.

Wang, A. P., S. Zhang, J. Xie, L. L. Gu, S. Wu, Z. Wu, L. Liu, Q. Feng, H. Y. Dong, and S. Y. Zhu. 2021. Isolation and characterization of a goose astrovirus 1 strain causing fatal gout in goslings, China. Poult. Sci. 100:101432.

Wang, H., Y. Zhu, W. Ye, J. Hua, L. Chen, Z. Ni, T. Yun, E. Bao, and C. Zhang. 2022a. Genomic and epidemiological characteristics provide insights into the phylogeographic spread of goose astrovirus in China. Transbound. Emerg. Dis. 69:e1865–e1876.

Wang, Y., C. Bai, D. Zhang, K. Yang, Z. Yu, S. Jiang, K. Ge, and Y. Li. 2020. Genomic and phylogenetic characteristics of a novel goose astrovirus in Anhui Province, Central-Eastern China. Gene 756:144898.

Wang, Z., H. Chen, S. Gao, M. Song, Z. Shi, Z. Peng, Q. Jin, L. Zhao, H. Qiao, C. Bian, X. Yang, X. Zhang, and J. Zhao. 2022b. Core antigenic advantage domain-based ELISA to detect antibody against novel goose astrovirus in breeding geese. Appl. Microbiol. Biotechnol. 106:2053–2062.

Wei, F., J. Yang, D. He, Y. Diao, and Y. Tang. 2020a. Evidence of vertical transmission of novel astrovirus virus in goose. Vet. Microbiol. 244:108657.

Wei, F., J. Yang, Y. Wang, H. Chen, Y. Diao, and Y. Tang. 2020b. Isolation and characterization of a duck-origin goose astrovirus in China. Emerg. Microbes. Infect. 9:1046–1054.

Wu, W., S. Qiu, H. Huang, R. Xu, E. Bao, and Y. Lv. 2021. Immune-related gene expression in the kidneys and spleens of goslings infected with goose nephritic astrovirus. Poult. Sci. 100:100990.

Wu, W., R. Xu, Y. Lv, and E. Bao. 2020. Goose astrovirus infection affects uric acid production and excretion in goslings. Poult. Sci. 99:1967–1974.

Xi, Y., Y. Huang, Y. Li, Y. Huang, J. Yan, and Z. Shi. 2022. The effects of dietary protein and fiber levels on growth performance, gout occurrence, intestinal microbial communities, and immunoregulation in the gut-kidney axis of goslings. Poult. Sci. 101:101780.

Xi, Y., J. Yan, M. Li, S. Ying, and Z. Shi. 2019. Gut microbiota dysbiosis increases the risk of visceral gout in goslings through translocation of gut-derived lipopolysaccharide. Poult. Sci. 98:5361–5373.

Xu, D., C. Li, G. Liu, Z. Chen, and R. Jia. 2019. Generation and evaluation of a recombinant goose origin Newcastle disease virus expressing Cap protein of goose origin avastrovirus as a bivalent vaccine in goslings. Poult. Sci. 98:4426–4432.

Xu, L., B. Jiang, Y. Cheng, Z. Gao, Y. He, Z. Wu, M. Wang, R. Jia, D. Zhu, M. Liu, X. Zhao, Q. Yang, Y. Wu, S. Zhang, J. Huang, X. Ou, Q. Gao, D. Sun, A. Cheng, and S. Chen. 2023a. Molecular epidemiology and virulence of goose astroviruses genotype-2 with different internal gene sequences. Front. Microbiol. 14:1301861.

Xu, L., B. Jiang, Y. Cheng, Y. He, Z. Wu, M. Wang, R. Jia, D. Zhu, M. Liu, X. Zhao, Q. Yang, Y. Wu, S. Zhang, J. Huang, S. Mao, X. Ou, Q. Gao, D. Sun, A. Cheng, and S. Chen. 2023b. Infection and innate immune mechanism of goose astrovirus. Front. Microbiol. 14:1121763.

Yang, J., J. Tian, Y. Tang, and Y. Diao. 2018. Isolation and genomic characterization of gosling gout caused by a novel goose astrovirus. Transbound. Emerg. Dis. 65:1689–1696.

Yin, D., J. Tian, J. Yang, Y. Tang, and Y. Diao. 2021. Pathogenicity of novel goose-origin astrovirus causing gout in goslings. BMC. Vet. Res. 17:40.

Yuan, X., K. Meng, Y. Zhang, L. Qi, W. Ai, and Y. Wang. 2018. Establishment and application of rapid diagnosis for reverse transcription-quantitative PCR of newly emerging goose-origin nephrotic astrovirus in China. mSphere 3:e00380-18.

Yuan, X., K. Meng, Y. Zhang, Z. Yu, W. Ai, and Y. Wang. 2019. Genome analysis of newly emerging goose-origin nephrotic astrovirus in China reveals it belongs to a novel genetically distinct astrovirus. Infect. Genet. Evol. 67:1–6.

Zhang, F., H. Li, Q. Wei, Q. Xie, Y. Zeng, C. Wu, Q. Yang, J. Tan, M. Tan, and Z. Kang. 2022a. Isolation and phylogenetic analysis of goose astrovirus type 1 from goslings with gout in Jiangxi province, China. Poult. Sci. 101:101800.

Zhang, M., X. Lv, B. Wang, S. Yu, Q. Lu, Y. Kan, X. Wang, B. Jia, Z. Bi, Q. Wang, Y. Zhu, and G. Wang. 2022b. Development of a potential diagnostic monoclonal antibody against capsid spike protein VP27 of the novel goose astrovirus. Poult. Sci. 101:101680.

Zhang, Q., Y. Cao, J. Wang, G. Fu, M. Sun, L. Zhang, L. Meng, G. Cui, Y. Huang, X. Hu, and J. Su. 2018a. Isolation and characterization of an astrovirus causing fatal visceral gout in domestic goslings. Emerg. Microbes. Infect. 7:71.

Zhang, X., T. Deng, Y. Song, J. Liu, Z. Jiang, Z. Peng, Y. Guo, L. Yang, H. Qiao, Y. Xia, X. Li, Z. Wang, and C. Bian. 2022c. Identification and genomic characterization of emerging goose astrovirus in central China, 2020. Transbound. Emerg. Dis. 69:1046–1055.

Zhang, X., D. Ren, T. Li, H. Zhou, X. Liu, X. Wang, H. Lu, W. Gao, Y. Wang, X. Zou, H. Sun, and J. Ye. 2018b. An emerging novel goose astrovirus associated with gosling gout disease, China. Emerg. Microbes. Infect. 7:152.

Zhang, Y., F. Wang, N. Liu, L. Yang, and D. Zhang. 2017. Complete genome sequence of a novel avastrovirus in goose. Arch. Virol. 162:2135–2139.

Zhu, Q., Y. Miao, J. Wang, W. Bai, X. Yang, S. Yu, D. Guo, and D. Sun. 2022. Isolation, identification, and pathogenicity of a goose astrovirus causing fatal gout in goslings. Vet. Microbiol. 274:109570.

Zhu, Q., and D. Sun. 2022. Goose astrovirus in China: a comprehensive review. Viruses. 14:1759.